Singlet-Groundstate Magnetism in TbP

I. Static Magnetic Properties*

J. Kötzler[1], G. Raffius[1], A. Loidl[2], and C.M.E. Zeyen[3]
[1] Institut für Festkörperphysik, Fachgebiet Technische Physik,
Technische Hochschule Darmstadt, Darmstadt, Federal Republic of Germany
[2] Institut für Physik, Johannes-Gutenberg-Universität, Mainz,
Federal Republic of Germany
[3] Institut Laue-Langevin, Grenoble, France

Elastic neutron scattering and magnetic susceptibility data are reported for temperatures around the Neél-point, $T_N = 7.3$ K, and for zero magnetic field. Above T_N, the temperature dependence of the magnetic central peak intensity can adequately be described within the RPA assuming isotropic exchange between nearest and next-nearest neighbours as the only parameters. This two-parameter model is quantitatively confirmed by the susceptibility data. At T_N, magnetic Bragg-intensities arise almost discontinuously (reaching 70% of the saturation within 0.1 K) accompanied by thermal hysteresis. For all temperatures below T_N the sublattice magnetic moment is explained by solutions of meanfield equations, if an effective quadrupole-quadrupole interaction is included. The quadrupolar coupling parameter is fully consistent with a value determined recently from the softening of the c_{44}-mode. These results show, that earlier suggestions of renormalization group results upon the origin of the first order phase transition in TbP are not needed.

1. Introduction

Terbium phosphide is an intermetallic compound of simple rocksalt structure. After the discovery of the transition to type II – antiferromagnetism at $T_N \approx 8$ K [1] the magnetic and elastic properties of TbP have attracted considerable experimental and theoretical interest. The Tb^{3+}-moments were found to be aligned parallel to the cube diagonals in accordance with crystal field calculations [2, 3]. Below T_N, two of the possible eight directions for the moment are stabilized by a rhombohedral distortion of the unit cell [4] accompanying the magnetic transition [5]. A sizable softening of the c_{44}-elastic constant observed above the ordering temperature was associated to effective quadrupole-quadrupole interactions mediated by conduction electrons [5].

More recently, an increasing interest of the magnetic behaviour of TbP has mainly arisen from two directions. First, this material is assumed to belong to a class of antiferromagnets being characterized by a large number of degrees of freedom for the order parameter ($n=4$ for TbP). Then, strong fluctuations are expected and renormalization group (RG) considerations, based on the non-existance of a stable fixed point, predict that the phase change is driven to first order [6, 7] though the Landau theory would predict a continuous transition. Detailed experimental checks of the RG-result, however, have to clear up whether other mechanisms (e.g. magnetostriction, multipole interactions, induced moment into singlet ground state), leading also to discontinuous transitions, are present in the magnet under investigation. In the case of TbP, the first order nature has been seen in the specific heat [5], but in order to elucidate

* A project of the Sonderforschungsbereich 65 "Festkörperspektroskopie" Darmstadt-Frankfurt, supported by the Deutsche Forschungsgemeinschaft

its origin, more detailed information on the magnetic properties is clearly desirable. This is one intention of this paper.

A second interesting feature of TbP is related to the nonmagnetic singlet ground state (Γ_1) of the Tb^{3+} in the octahedral crystal field [8]. Since the energy of the first excited state ($E(\Gamma_4)=18.9\ k_B\cdot K$ [5]) exceeds $k_B T_N$ strong ion-ion interactions must be operative to induce the magnetic phase transition and the moment of 6.2 (3) μ_B [1, 2]. From RPA calculations it is expected that a continuous transition in such system is driven by a divergent central mode associated with the Curie susceptibility of the excited states in the J-multiplet. The increasing central peak intensity, if T_N is approached from the paramagnetic side [9, 10], should be accompanied by a softening of the transverse mode developing from the crystal field excitation. From the experimental part, these dynamic aspects of singlet ground state magnets are still inconclusive [10, 11] and, therefore, further investigations on single crystals of such systems have been suggested. Part II of this work [12] reports on inelastic neutron scattering from TbP. Some results of this work were communicated to us prior to the present investigation by K. Knorr (Mainz) and A. Loidl showing the discontinuous onset of the magnetic order parameter at T_N and the existence of a central peak around the L-Point.

Finally we recall, that the existence of a singlet ground state may also be responsible for a first order transition. Within the mean field approximation it was already shown for some special cases that, depending on the relative strength of exchange to crystal field interaction, there may be a second or first order or no transition [13].

The remainder of this paper is organized as follows. After giving some experimental details in Sect. 2, we report and discuss (within the RPA) the results of the elastic diffuse neutron scattering (Sect. 3A) and the homogeneous susceptibility (Sect. 3B). The results on the sublattice magnetization are presented in Sect. 4A, being followed by a quantitative discussion by help of selfconsistent mean field equations (Sect. 4B). Section 5 containing our summary and conclusions completes this work.

2. Experimental

All TbP samples investigated here were prepared from the same charge*. In the neutron diffraction study we used a single crystal (mosaic spread 10′) of about 0.5 cm^3, containing spurious amounts of additional deorientated crystallites. The susceptibility measurements were carried out on a powder specimen.

The neutron scattering was measured at the three-axis diffractometer D 10 A of the ILL at Grenoble. Thermal neutrons incident from the H24 guide tube were vertically focused on the sample by a Cu(200) monochromator ($\lambda=1.26$ Å). All scans were carried out in the (hll) plane of TbP. The integrated intensities I_N and I_M of nuclear and magnetic reflections, respectively, were evaluated by help of a routine developed by M.S. Lehmann (Grenoble). Above the ordering temperature the diffuse scattered neutrons were analyzed by means of a curved (008) pyrolytic graphite crystal. This way inelastic scattering arising from the excitations ($\Delta E \geqq 0.4$ meV [12]) was eliminated so that the measured $\mathbf{q}$-dependent intensities could rather safely be attributed to the central peak. – The low temperatures of the sample were produced by a He-flow cryostat. Near T_N the temperatures were stabilized within ± 1 mK.

The measurements of the homogeneous ($\mathbf{q}=0$) susceptibility were carried out in the earth's field (30 μT) by a SQUID magnetometer. The gradiometer coils were wound on a vacuum chamber containing the sample encapsulated by a copper sample holder and being in close thermal contact with the Ge-thermometer. The temperature could be varied from 4 to 100 K. More details on this arrangement will be published elsewhere [14].

* We are much indebted to E. Bucher for providing us with the TbP

3. Magnetic Properties Above T_N

A. Diffuse Magnetic Scattering

Approaching T_N from the paramagnetic region, strong diffuse neutron scattering occurs around the magnetic Bragg points. Figure 1a, b shows results of scans parallel to the $[(4-h)hh]$- and $[h00]$-directions through the most intense (311) reflection. As mentioned above, these data should correspond to the (energy-)integrated intensities of the central mode, $S_0(\mathbf{q})$, where the wavevector $\mathbf{q}$ stands for the deviation of the scattering vector $\mathbf{Q}$ from the magnetic Bragg point τ_M (τ_M is given in units of the magnetic cell).

For identical moments J experiencing isotropic exchange and crystal field interactions,

$$\mathcal{H}=\sum_i V_{cf}(i)-\tfrac{1}{2}\sum_{ij}\mathcal{J}(ij)\,\mathbf{J}(i)\cdot\mathbf{J}(j),$$

Buyers [10] has calculated the structure factor of the central peak within the RPA:

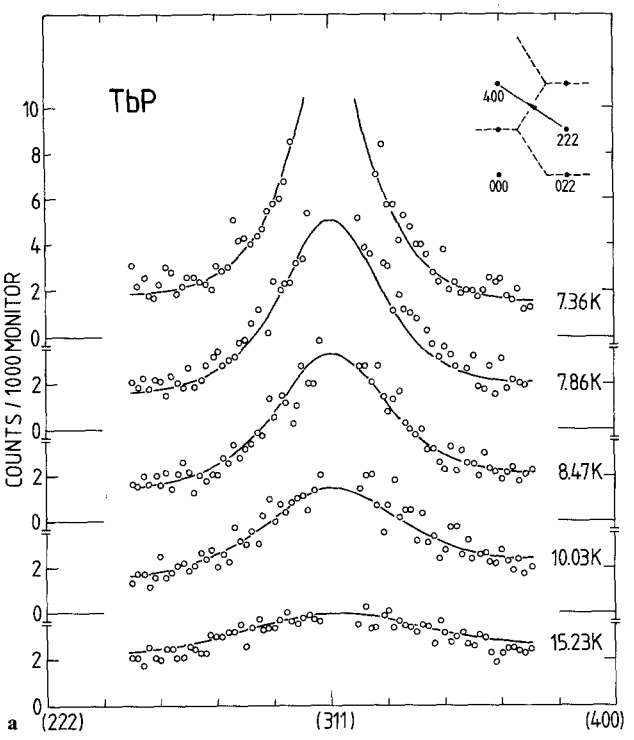

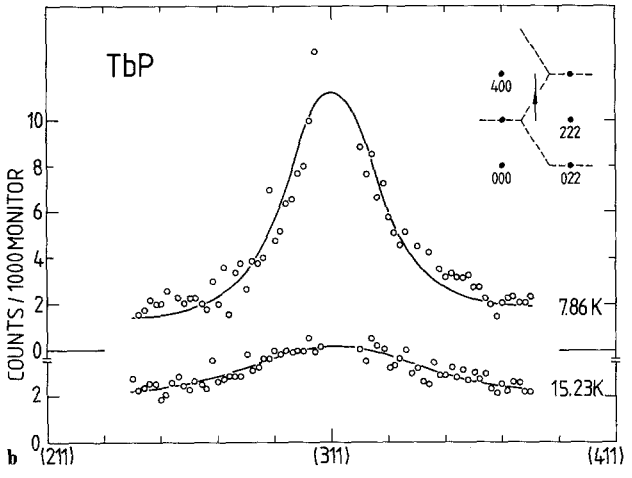

Fig. 1a and b. Neutron diffraction scans through the magnetic (311)-reflection along two different directions (shown by the inserts to Figs. a and b) for temperatures $T \gtrsim T_N$. Solid lines represent fits to the RPA model (Eq. 1) described in the text. A small Bragg-spike probably originating from impurities is not considered (spike intensity at 8.5 K is less than 10^{-3} of saturation intensity for the bulk.)

$$S_0(\mathbf{q}) = \frac{g_0(T) - g_v(T)}{1 - \mathcal{J}(\mathbf{q}) \cdot g_v(T)} \cdot \frac{k_B T}{1 - \mathcal{J}(\mathbf{q}) \cdot g_0(T)} \tag{1}$$

$\mathcal{J}(\mathbf{q}) = \sum_j \mathcal{J}(ij) \cdot \exp[i\mathbf{q} \cdot (\mathbf{r}_i - \mathbf{r}_j)]$ denotes the Fourier-transform of the exchange interaction, and g_0 and g_v are proportional to the total ionic and van Vleck susceptibilities, respectively:

$$g_0 = \frac{\chi_0}{\lambda} = \sum_{n_0 m_0} \frac{|\langle n_0 | J_z m_0 \rangle|^2}{E_{m_0} - E_{n_0}} \frac{e^{-\frac{E_{n_0}}{k_B T}} - e^{-\frac{E_{m_0}}{k_B T}}}{Z_0} \tag{2a}$$

$$g_v = \frac{\chi_v}{\lambda} = \sum_{m_0 \neq n_0} \frac{|\langle m_0 | J_z n_0 \rangle|^2}{E_{m_0} - E_{n_0}} \frac{e^{-\frac{E_{n_0}}{k_B T}} - e^{-\frac{E_{m_0}}{k_B T}}}{Z_0} \tag{2b}$$

where $\lambda = (g_J \mu_B)^2 / v_{\text{spin}}$. n_0 denote eigenstates and -values of the crystal-field Hamiltonian. For TbP Birgeneau et al. [15] found $B_6^0 = 0$, and so we take with z along the (111) direction:

$$V_{\text{cf}} = -\tfrac{2}{3} \beta_J B_4^0 (O_4^0 - 20\sqrt{2}\, O_4^3), \tag{3}$$

where $\beta_J = 1.22 \cdot 10^{-4}$ and $Z_0 = \sum_{n_0} \exp(-E_{n_0}/k_B T)$ is the partition sum of one ion.

In the analysis of the measured intensities $I(\mathbf{q})$ around (311), resolution corrections proved to be unnecessary, since the width of the most narrow diffuse scattering (at 7.4 K) was found to be a factor of seven larger than that of the resolution function of the diffractometer. Thus, after subtracting a background, I_B, common to all seven scans, we can relate the measured intensities directly to the structure factor introducing a scale factor as second instrumental parameter: $I(\mathbf{q}) = A_1 \cdot S_0(\mathbf{q}) + I_B$. Assuming for the crystal field parameter the value of Bucher et al. [5], $B_4^0 = 7.4$ meV, we are left with the determination of the exchange constants $\mathcal{J}(ij)$, when comparing the measured diffuse scattering to the RPA theory, Eq. (1). Following Busch et al. [16] and Holden et al. [17], who proposed to consider the exchange between nearest and next-nearest neighbours in TbP and TbSb, respectively, we have introduced these two physical parameters, $\mathcal{J}(1n)$ and $\mathcal{J}(2n)$, besides the two instrumental ones (A_1 and I_B) into the fit. The results are indicated by solid lines into Fig. 1, showing a satisfactory overall agreement, regarding the fact that only four adjustable parameters are involved. Thus, the RPA model appears to work quite well for TbP even near T_N, which is plausible because the strong first order nature of this transition (to be shown in Sect. 3) suppresses the formation of critical fluctuations. The quality of the applied model becomes also evident from the small standard errors for the exchange constants being listed in Table 1 together with previously published values. Though the signs of the exchange agree, there are some discrepancies which will be discussed below (Sect. 5). Finally we note, that K. Knorr directing our attention to Eq. (1), provided a preliminary fit of the T-and-$\mathbf{q}$-dependence of our data using exchange parameters

Table 1. Exchange interactions in TbP between nearest and next-nearest neighbours deduced in this work from diffuse neutron scattering. Exchange sums, $\mathcal{J}(\mathbf{q}=0)$ are determined from homogeneous susceptibility ($\mathcal{J}_s$) and the neutron data ($\mathcal{J}_n = 12\mathcal{J}(1n) + 6\mathcal{J}(2n)$)

Ref.	This work	22	1,2
$\mathcal{J}(1n)$	7.35(13)	8.6	–
$\mathcal{J}(2n)$	−10.37(3)	−15.5	−14.5(1.5)
$\mathcal{J}_s(\mathbf{q}=0)$	24.4(2)	10.2	–
$\mathcal{J}_n(\mathbf{q}=0)$	26.0(1.8)	–	–

extracted from the dispersion of the magnetic excitations (s. part II [12]).

B. Zero-Field Susceptibility

The results of the SQUID-measurements between 5 K and 75 K are displayed in Fig. 2. The finite cusp of the homogeneous susceptibility at $T_N = 7.30$ K is characteristic for the absence of a spontaneous magnetic moment. Obviously (s. insert to Fig. 2) the data can be well described by the mean field approximation (MFA)

$$\frac{1}{\chi(T)} = \frac{1}{\chi_0(T)} + \frac{\mathcal{J}(\mathbf{q}=0)}{\lambda}. \tag{4}$$

Taking $\lambda = (g_J \mu_B)^2 / v_{\text{spin}} = 33.18$ μeV for TbP we find from the intercept of χ^{-1} with the abcissa $\mathcal{J}(\mathbf{q}=0) = 24.4(2)$ μeV as compared to $\mathcal{J}(\mathbf{q}=0) = 12\ \mathcal{J}(1n) + 6\mathcal{J}(2n) = 26.0(1.8)$ μeV following with the exchange parameters deduced from the diffuse scattering (s. Fig. 1 and Table 1). We believe that this result also favours the exchange constants of this work over those of Ref. 16 which would lead to $\mathcal{J}(\mathbf{q}=0) = 10.2$ μeV.

4. Sublattice Magnetic Moment

A. Experimental Results

TbP crystallizes in the rocksalt structure and its magnetic structure belongs to the class of type II – antiferromagnets consisting of alternating ferromagnetic (111) sheets. The Tb moments are aligned along [111]-directions leading to the formation of four types of domains defined by different spin directions, say [111], [$\bar{1}$11], [1$\bar{1}$1], and [11$\bar{1}$].

The intensity for unpolarized neutrons scattered at a Braggpoint $\tau = (hkl)$ of a material containing identical moments μ is given by the well-known expression [18]

$$I(\tau, \mu) = \frac{A}{\sin 2\Theta} [|F_N(\tau)|^2 + |F_M(\tau)|^2] \cdot E(\tau, \mu, T). \tag{5}$$

Here A denotes the scale factor and 2Θ is the scattering angle and τ is given in units of the magnetic cell. The factor $E \leqq 1$ accounts for possible thermal and

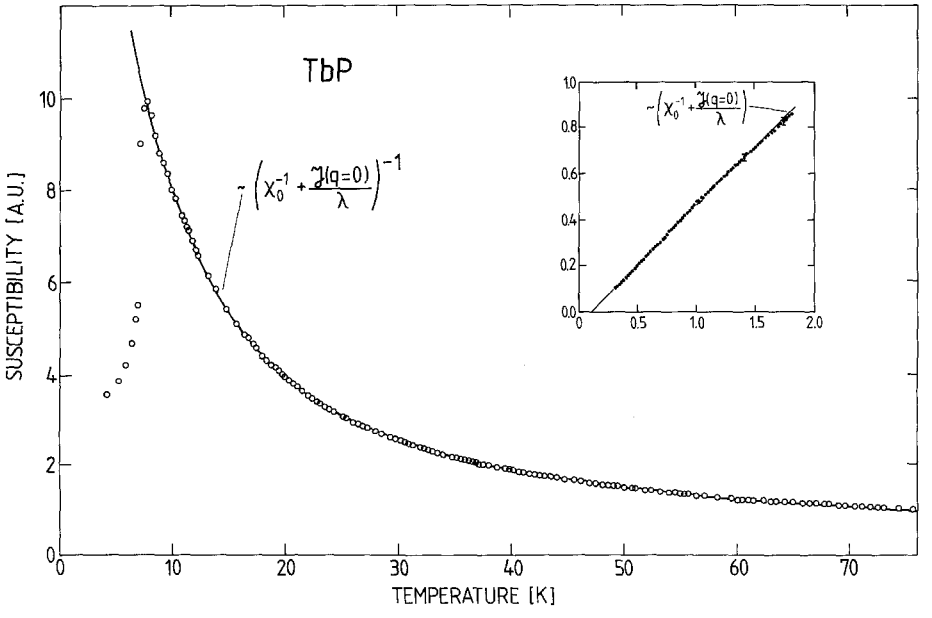

Fig. 2. Magnetic susceptibility of TbP in zero magnetic field. Full line shows the adjustment to the MFA (Eq. 4)

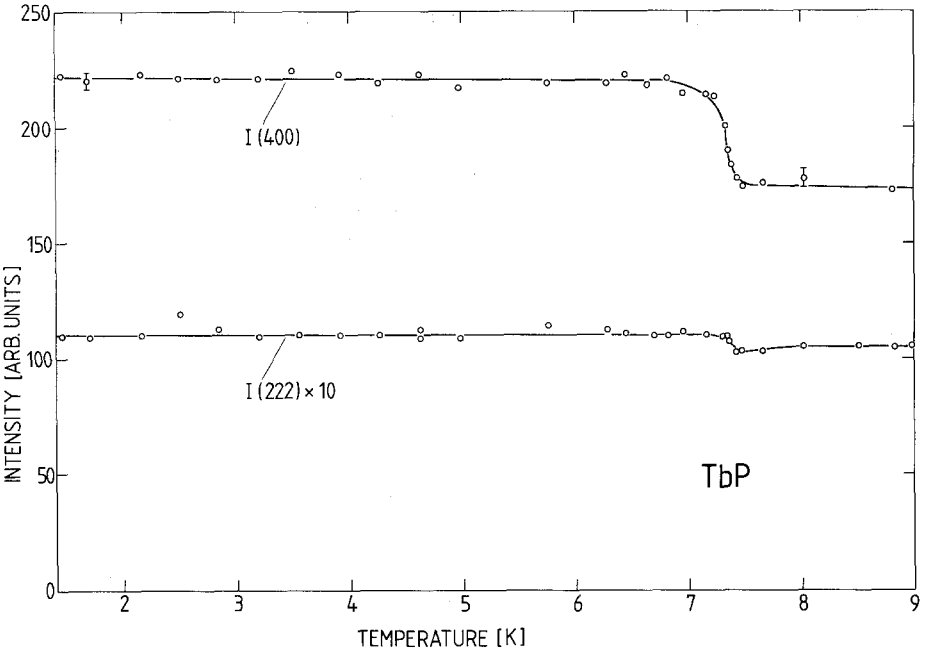

Fig. 3. Integrated neutron diffraction intensities of a strong and a weak nuclear reflection (s. Eqs. (6a), (6b)) vs. temperature. The change of intensity occurs at the magnetic transition (s. Fig. 4). Full lines are drawn as guides to the eye

extinction corrections. The non-vanishing nuclear amplitudes for the NaCl structure produce either strong or weak reflections:

$$F_N(\tau)=32(b_{\mathrm{Tb}}+b_{\mathrm{P}}), \quad \text{if } h+k+l=4n, \tag{6a}$$

$$=32(b_{\mathrm{Tb}}-b_{\mathrm{P}}), \quad \text{if } h+k+l=4n+2, \tag{6b}$$

where $b_{\mathrm{Tb}}=7.6\,\mathrm{fm}$ and $b_{\mathrm{P}}=5.1\,\mathrm{fm}$ are the coherent nuclear scattering lengths of the constituents for thermal neutrons [19]. The magnetic structure factor for the magnetic unit cell of a type II – antiferromagnet assumes only one non-zero value [20]:

$$F_M(\tau,\mu)=32p_{\mathrm{Tb}}(\mu,\tau), \quad \text{if } h,k,l \text{ are all odd,}$$
$$\text{and } h+k,\ k+l,\ l+h=4n+2. \tag{7}$$

p_{Tb} represents the magnetic scattering length per Tb^{3+}:

$$p_{\mathrm{Tb}}(\mu,\tau)=2.696 f_{\mathrm{Tb}}(\tau)\cdot\frac{\mu}{\mu_B}\cdot\left(1-\left(\frac{\mu}{\mu}\cdot\frac{\tau}{\tau}\right)^2\right)^{1/2}, \tag{8}$$

which except for μ depends on the magnetic form factor of Tb [21] and on the angle between the scattering vector τ and the magnetic moment. This projection factor forbids for TbP magnetic Bragg scattering for τ being parallel to one of the four cube diagonals, {111}.

Among the four different domains only two, defined by spin directions [111] and [$\bar{1}$11], exhibit reflections in the (hll)-scattering plane chosen in our experiment. According to Eqs. (7), (8), the strongest magnetic intensity arises from the ($\bar{3}$11)-Bragg-point in the ($\bar{1}$11)-domain, while the (111)-domain does not contribute. In general, all reflections observable in the (hll)-plane originate either from the (111)- or the ($\bar{1}$11) domains. Assuming all domains to be equally populated, the magnetic scattering intensities in the (hll)-plane of TbP should take the values:

$$I_M(\tau,\mu)=\frac{A}{\sin 2\Theta}\cdot(16p_{\mathrm{Tb}}(\tau,\mu))^2. \tag{9}$$

Here we have set $E=1$, ignoring thermal and extinction corrections because of the low temperatures ($<7.3\,\mathrm{K}$) and moderate magnetic scattering intensities.

In order to determine the absolute value of the magnetic moment from the measured intensities we calculated the scale factor A from the nuclear intensities. For this purpose we only employed the weak reflections, Eq. (6b), because the strong ones (Eq. 6a) appear to suffer by extinction. This is illustrated in Fig. 3 representing one example of both groups. At $T_N=7.3\,\mathrm{K}$ the intensity of (400) and all other strong reflections exhibit a jump of about 20%, while for the weak reflections the change is insignificant. It is plausible to attribute this effect to primary extinction (being independent on $\sin 2\Theta$ [22]), which to a great extent is suppressed below T_N due to the formation of the four crystallographic domains discussed above. By a rough estimate of the domain size, using a formula for spherically shaped domains [22], we obtain from E

Table 2. Nuclear and magnetic Bragg intensities of TbP($T_N = 7.3$ K) measured at 1.5 K. Weak nuclear reflections serve to determine the scale factor A, by which the moment μ is calculated from the magnetic intensities

τ_N	$I_N \cdot \sin 2\Theta$ [a.u.]	$A\left[\frac{\text{a.u.}}{\text{fm}^2}\right]$	τ_M	$I_M \cdot \sin 2\Theta$ [a.u.]	$\mu(1.5\,\text{K})[\mu_B]$
222	41.6	6.5	$\bar{3}11$	453.8	6.99
622	42.9	6.7	$\bar{1}33$	189.8	6.47
266	40.4	6.3	$\bar{5}33$	234.1	6.49
400	953.9	(5.8)	$\bar{3}55$	140.8	6.58
444	952.3	(5.8)	733	31.7	6.87

$= 0.8$ for our TbP sample a diameter of 21 μm. In Table 2 we have compiled the largest intensities among the strong and weak reflections, corrected for the Lorentz-factor. The scale factors A were determined according to Eq. (5), and it can be seen that even in the domain region where I_N has been measured (1.5 K), the extinction cannot be completely ignored for the strong reflections. Thus we are forced to determine a mean value for A from the weak nuclear intensities alone. It is then straightforward to calculate the magnetic moment μ from I_M using Eqs. (5), (8) and (9). As the mean of these results we find for the magnetic moment $\mu(1.5\,\text{K}) = 6.68$ (23) μ_B, which should be very close to the saturation value in zero field. This moment is somewhat larger than the 6.2(3) μ_B following from powder diffraction data [1, 2] and is considerably smaller than the maximum value of the free ion, $9\mu_B$, which can be reached only in high magnetic fields ($B > 13$ T [16]) due to the strong crystal field effect.

The influence of temperature on the magnetic moment is shown by Fig. 4. The steep decrease around $T_N = 7.3$ K amounting to 70 % within 0.15 K, and also the thermal hysteresis shown by the insert leads us to conclude that the phase transition in TbP is strongly of first order. This is consistent with the observation of a latent heat by Bucher et al. [5].

B. Selfconsistent Calculations

With regard to the success of the mean-field type approximation explaining the magnetic properties of TbP above the Neél temperature, it is near at hand to apply the MFA also below T_N. In order to calculate the spontaneous momentum in a sublattice we start from the following MFA-Hamiltonian:

$$\mathcal{H}_{\text{MFA}}(i) = V_{\text{cf}}(i) - \mathcal{J}_{\text{AF}} \langle J_z \rangle J_z(i) - \mathcal{K}_0 \langle Q_z \rangle Q_z(i)$$

where z is defined by the cube diagonal. Except for the crystal field and exchange interactions, already introduced above to discuss the paramagnetic behaviour above T_N, we take account also of an effective quadrupole-quadrupole interaction ($Q_z = J_z^2 - J(J+1)/3$ s.e.g. review by Gehring and Gehring [23]) to describe cooperative Jahn-Teller effects. $\mathcal{K}_0$ corresponds to the ferrodistortive quadrupolar coupling at the Γ point

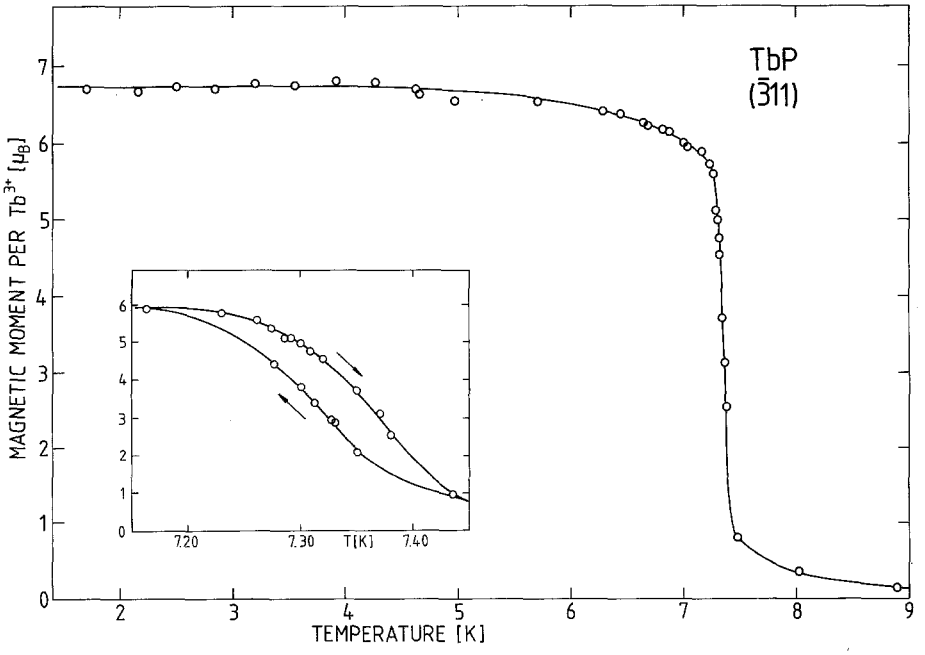

Fig. 4. Sublattice magnetic moment of TbP derived from the ($\bar{3}11$) reflection. The measurement was started at low temperatures. Insert shows also the cooling curve. Full lines serve as guides to the eye

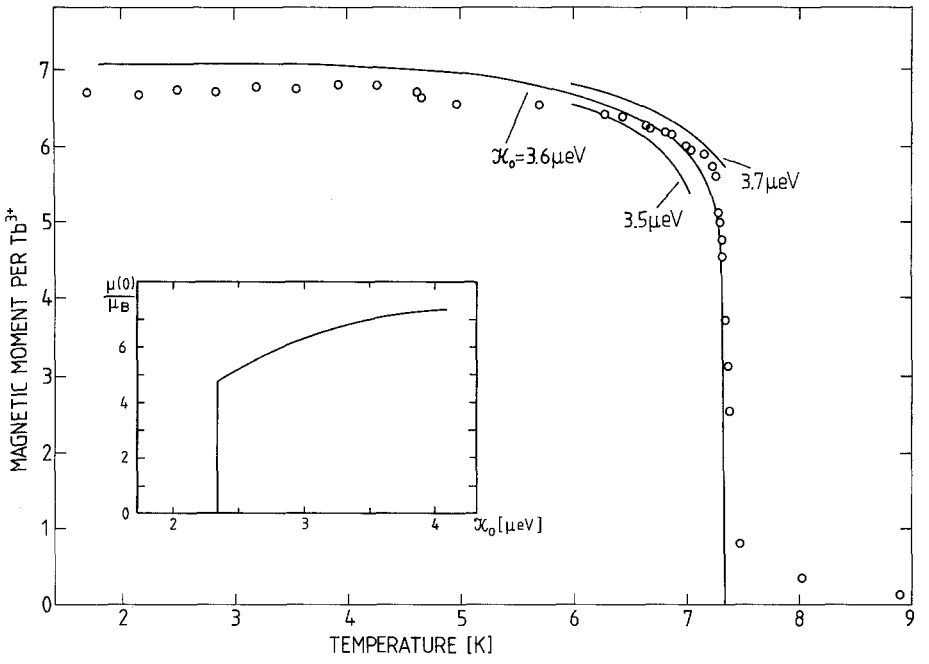

Fig. 5. Comparison between experimental sublattice magnetic moment and MFA-results using the interaction parameter $\mathcal{J}_{AF}=52.2\,\mu eV$ determined in this work. The strong effect of the effective quadrupolar coupling $\mathcal{K}_0$ on the saturation moment and on T_N is evident

containing contributions from both interactions between the electric quadrupole moments (g') and magneto-elastic coupling (g_3^2). For TbP these coupling constants have been determined by Bucher et al. [5] by analyzing the softening of the c_{44}-mode. They find $g'=1.12(2)$ μeV and $g_3^2=0.085(17)$ μeV, from which follows $\mathcal{K}_0=3(g_3^2+g')=3.6(6)$ μeV (the prefactor 3 arises from the fact that our interaction operator is smaller by a factor of 3 than that underlying the formula for c_{44} used in Ref. 5). $\mathcal{J}_{AF}$ denotes the antiferromagnetic coupling at the L point taking the value $\mathcal{J}_{AF}=-6\mathcal{J}(2n)+\mathcal{J}_{AF}(\text{dip})=52.2(2)$ μeV, because in the ordered phase of a type II-antiferromagnet the contributions of the next-nearest neighbours, one half of which is aligned ferromagnetically, cancel each other.

Using this MFA-Hamiltonian we calculated selfconsistently by means of iterative procedures energies and eigenvalues for $J=6$ from

$$\mathcal{H}_{MFA}|n\rangle=E_n|n\rangle$$

with the dipolar moment in one sublattice:

$$\langle J_z\rangle=\sum_n\langle n|J_z n\rangle\cdot\exp(-E_n/k_BT)$$

and the quadrupolar moment

$$\langle Q_z\rangle=\sum_n\langle n|Q_z n\rangle\cdot\exp(-E_n/k_BT)$$

where $Z=\sum_n\exp(-E_n/k_BT)$. The results of the computations employing double precision routines are displayed by Fig. 5. We find excellent agreement with the experimental data even near T_N if we assume an effective quadrupolar coupling of $\mathcal{K}_0=3.6\,\mu eV$. This value is fully consistent with $\mathcal{K}_0=3.6(6)\,\mu eV$ derived from the ultrasonic data. This quadrupolar coupling is too weak to induce by itself a structural transition, but it exerts a great effect on the magnetic transition. As is illustrated by the insert to Fig. 5 the transition disappears at $\mathcal{K}_0=2.3\,\mu eV$, and moreover in the region of interest the saturation moment depend strongly on $\mathcal{K}_0$. A more detailed discussion of the thermodynamic properties of the phase-transition in TbP and related compounds will be given elsewhere [24].

5. Conclusions

The measurements of the sublattice moment of the singlet-groundstate system TbP show that the antiferromagnetic transition at $T_N=7.30$ K is strongly of first order. The temperature dependence of the moment can be explained by selfconsistent solutions of mean field equations using the full level scheme of Tb^{3+}, if besides an isotropic exchange interaction an effective quadrupole-quadrupole coupling $\mathcal{K}_0$ is included. $\mathcal{K}_0=3.6$ μeV agrees excellent with $3.6(\pm0.6)$ μeV determined previously from ultrasonic data [5]. The exchange interactions between nearest and next-nearest neigh-

bours in TbP could be evaluated to a great accuracy from the diffuse neutron scattering above T_N, since these results proved to be fully consistent with the RPA-result of Buyers [10]. Moreover, the results on the homogeneous susceptibility confirmed the proposed exchange model. The selfconsistent calculations reveal the strong influence of the quadrupolar coupling $\mathscr{K}_0$ on the saturation moment as well as on the Neél temperature. It is very likely that this effect is responsible for the discrepancy between the exchange parameters of this work and those of Ref. [16]. There the quadrupolar coupling was ignored in the analysis of magnetization measurements. The magnetic ordering could, therefore, only be accounted by a larger *nnn*-exchange, which was taken almost twice as large as our value (cp. Table 1).

From the fact that the static magnetic behaviour of TbP even in the immediate neighbourhood of T_N can be described by the mean field approximation, it follows that critical fluctuations are completely absent, which is plausible with regard to the strong first order nature of the transition. Thus, in contrast to earlier suggestions, TbP cannot serve as a check of *RG*-calculations [6, 7], predicting that a first order transition may simply arise from large fluctuations, which should occur in systems with a large number of degrees of freedom for the order parameter ($n=4$ for TbP, corresponding to the four cube diagonals for the moment direction). Consequently, our results show that considerable efforts are necessary to clear up whether in the magnets listed by Ref. [6, 7] other origins for a discontinuous transition exist (singlet groundstate, magnetoelastic or quadrupole couplings), before a firm conclusion about the effect of fluctuations on the order of the transition can be drawn.

In summary, we have reported the static behaviour of the order parameter and its susceptibility around the phase transition of a discontinuously ordering system and, to our knowledge for the first time, a quantitative description involving no adjustable parameter, was provided.

We thank E. Bucher for providing us with the TbP sample.
We are much indebted to B. Lüthi and K. Knorr (Mainz) for focusing our interest on TbP and for helpful discussions. Thanks are also due to J.K. Kjems (Risø), for comments on the first draft. This research was in part (A.L.) supported by the BMFT.

References

1. Child, H.R., Wilkinson, M.K., Cable, J.W., Koehler, W.C., Wollan, E.O.: Phys. Rev. **131**, 922 (1963)
2. Trammell, G.T.: Phys. Rev. **131**, 932 (1963)
3. Stevens, K.W.H., Pytte, E.: Solid State Commun. **13**, 101 (1973)
4. Lévy, F.: Phys. Kondens. Mat. **10**, 85 (1969)
5. Bucher, E., Maita, J.P., Hull, Jr. G.W., Longinotti, L.D., Lüthi, B., Wang, P.S.: Z. Physik B **25**, 41 (1976)
6. Mukamel, D., Krinsky, S.: Phys. Rev. B **13**, 5065, 5078 (1976)
7. Brazovskii, S.A., Dzyaloshinskii, I.E., Kukharenko, B.G.: Sov. Phys. JETP **43**, 1178 (1976)
8. Lea, K.R., Leask, M.J.M., Wolf, W.P.: J. Phys. Chem. Solids **23**, 1381 (1962)
9. Fulde, P., Peschl, I.: Adv. Phys. **21**, 1 (1972)
   Fulde, P. In: Handbook on the Physics and Chemistry of Rare Earth, Gscheidner, K.A., Eyring, L. (eds.) p. 296 (1978)
10. Buyers, W.J.L. In: Ann. Conf. on Magnetism and Magnetic Materials, San Francisco, Graham, C.D., Lander, G.H., Rhyne, J.J. (eds.) (AIP Conf. Proc. 24), 27 (1975)
11. Als-Nielsen, J., Kjems, J.K., Buyers, W.J.L., Birgeneau, R.J.: J. Phys. C **10**, 2673 (1977)
12. Knorr, K., Loidl, A., Kjems, K., Lüthi, B.: To be published
13. Blume, M.: Phys. Rev. **141**, 517 (1966)
    Wang, Y.L.: Solid State Commun. **10**, 533 (1972)
14. Frowein, R., Kötzler, J.: to be published
15. Birgeneau, R.J., Bucher, E., Maita, J.P., Passell, L., Turberfield, K.C.: Phys. Rev. B **8**, 5345 (1973)
16. Busch, G., Schwob, P., Vogt, O.: Phys. Lett. **11**, 100 (1964)
17. Holden, M.T., Svensson, E.C., Buyers, W.J.L., Vogt, O.: Phys. Rev. B **10**, 3864 (1974)
18. Bacon, G.E.: Neutron Diffraction, 3rd edition, Oxford: Clarendon Press 1975
19. Mughabghab, S.F., Garber, D.I.: BNL 325-Neutron cross sections: I 3rd edn (Upton: Brookhaven National Laboratory)
20. Roth, W.L.: Phys. Rev. **110**, 1333 (1958)
21. Steinsvoll, O., Shirane, G., Nathans, R., Blume, M., Alperin, H.A., Pickart, S.J.: Phys. Rev. **161**, 499 (1967)
22. Becker, P.J., Coppens, Ph.: Acta Crystallogr. A **30**, 129 and 148 (1974)
23. Gehring, G.A., Gehring, K.A.: Rep. Progr. Phys. **38**, 1 (1975)
24. Kötzler, J., Raffius, G.: to be published

J. Kötzler
G. Raffius
Institut für Festkörperphysik
Fachgebiet Physik
Technische Hochschule Darmstadt
Schloßgartenstraße
D-6100 Darmstadt
Federal Republic of Germany

A. Loidl
Institut für Physik
Johannes-Gutenberg-Universität
Postfach 3980
D-6500 Mainz
Federal Republic of Germany

C.M.E. Zeyen
Institut Max von Laue –
Paul Langevin
156 X Centre de Tri
F-38042 Grenoble Cédex
France